Introducing a New Triazoloquinoxaline-Based Fluorene Copolymer for Organic Photovoltaics: Synthesis, Characterization, and Photovoltaic Properties

Derya Baran,[1] Felix M. Pasker,[2] Stephan Le Blanc,[2] Gregor Schnakenburg,[3] Tayebeh Ameri,[1] Sigurd Höger,[2] Christoph J. Brabec[1,4]

[1]Institute of Materials for Electronics and Energy Technology, Department of Materials Science and Engineering, Friedrich-Alexander-University Erlangen-Nurnberg, Martensstrasse 7, Erlangen 91058, Germany
[2]Kekulé-Insitute of Organic Chemistry and Biochemistry, Rheinische Friedrich-Wilhems-University Bonn, Gerhard-Domagk-Str.1, Bonn 53121, Germany
[3]Insitute of Inorganic Chemistry, Rheinische Friedrich-Wilhems-University Bonn, Gerhard-Domagk-Str.1, Bonn 53121, Germany
[4]Bavarian Center for Applied Energy Research (ZAE Bayern), Am Weichselgarten 7, Erlangen 91058, Germany
Correspondence to: D. Baran (E-mail: derya.baran@ww.uni-erlangen.de); S. Höger (E-mail: hoeger@uni-bonn.de)

Received 10 September 2012; accepted 26 October 2012; published online 27 November 2012
DOI: 10.1002/pola.26465

ABSTRACT: A new donor-acceptor copolymer consisting of triazoloquinoxaline and 9,9-dialkylfluorene units on the main chain has been synthesized, characterized and evaluated as donor material in bulk heterojunction solar cells using $PC_{61}BM$ as an acceptor. The resulting polymer PTQF showed good thermal stability and solubility in common organic solvents. Cyclic Voltammetry measurements showed that the PTQF has HOMO–LUMO energy levels of −5.13 and −3.62 eV, respectively. DFT calculations revealed that the HOMO is delocalized all over the thiophene and fluorene units and the LUMO is localized mainly on the triazole and pyrazine units. PTQF absorbs broadly in the visible region and exhibits a bandgap of 1.4 eV. Photovoltaic devices exhibited 1.7% efficiency for 1:2 PTQF:$PC_{61}BM$ blend ratio using Ca/Ag electrodes. © 2012 Wiley Periodicals, Inc. J. Polym. Sci., Part A: Polym. Chem. **2013**, *51*, 987–992

KEYWORDS: conducting polymers; conjugated polymers; electrochemistry; organic photovoltaics; triazoloquinoxaline; fluorene copolymer; benzotriazole; Suzuki coupling

INTRODUCTION In the last decade, great effort has been used to improve the power conversion efficiencies (PCE) of polymeric solar cells (PSC), and efficiencies above 7% have been reported by many groups.[1–5] Fullerene derivatives have been proved as commonly used and most effective acceptor materials for organic photovoltaics. Therefore, several studies have been concentrated on designing new donor materials with low band gap and beneficial nanoscale morphology.[6] However, materials with narrow band gap sometimes suffer from low open-circuit voltage (V_{oc}) due to the built-in potential between HOMO energy of the donor ($HOMO_d$) and the LUMO energy of the acceptor ($LUMO_a$).[7] V_{oc} is one of the keys and limiting parameter to obtain high efficiency polymers, and it is proportional to the energy $HOMO_d$ and the $LUMO_a$. After extensive research, some design rules are summarized for efficient donor materials such as (i) a band gap around 1.5 eV, (ii) a balanced HOMO-LUMO energy for maximum V_{oc} and minimum LUMO offset to reduce energy losses, (iii) appropriate solubility and miscibility with fullerene derivatives.

Quinoxalines have already been successfully used as electron poor comonomers of low band gap polymers in PSCs.[8–12] 2,3-Diphenylquinoxaline is one of the most commonly investigated quinoxaline derivative due to its versatility and facile synthesis. Also thiadiazoloquinoxaline was used as comonomer with 9,9-dialkylfluorene to achieve high performances in photovoltaics.[13]

Recently, benzotriazole (BTz) containing oligomers and polymers have attracted considerable attention in organic photovoltaics due to their functionality.[14–21] Unlike benzothiadiazole (BTd), the benzotriazole moiety provides an advantage of incorporating alkyl chains or aryl substituents onto the acceptor unit, superior for keeping the polymer soluble. Power conversion efficiencies as high as 7% have been reached using BTz as donor comonomer for PSCs.[1]

On the basis of the rules and developments mentioned above, we designed a new monomer namely 6,7-bis(3-methoxyphenyl)-4,9-di(thiophen-2-yl)-2-(3,5-difluoro-4-(2-octyldodecyloxy)phenyl)-2H-triazolo[4,5-g]quinoxaline and copolymerized

Additional Supporting Information may be found in the online version of this article.

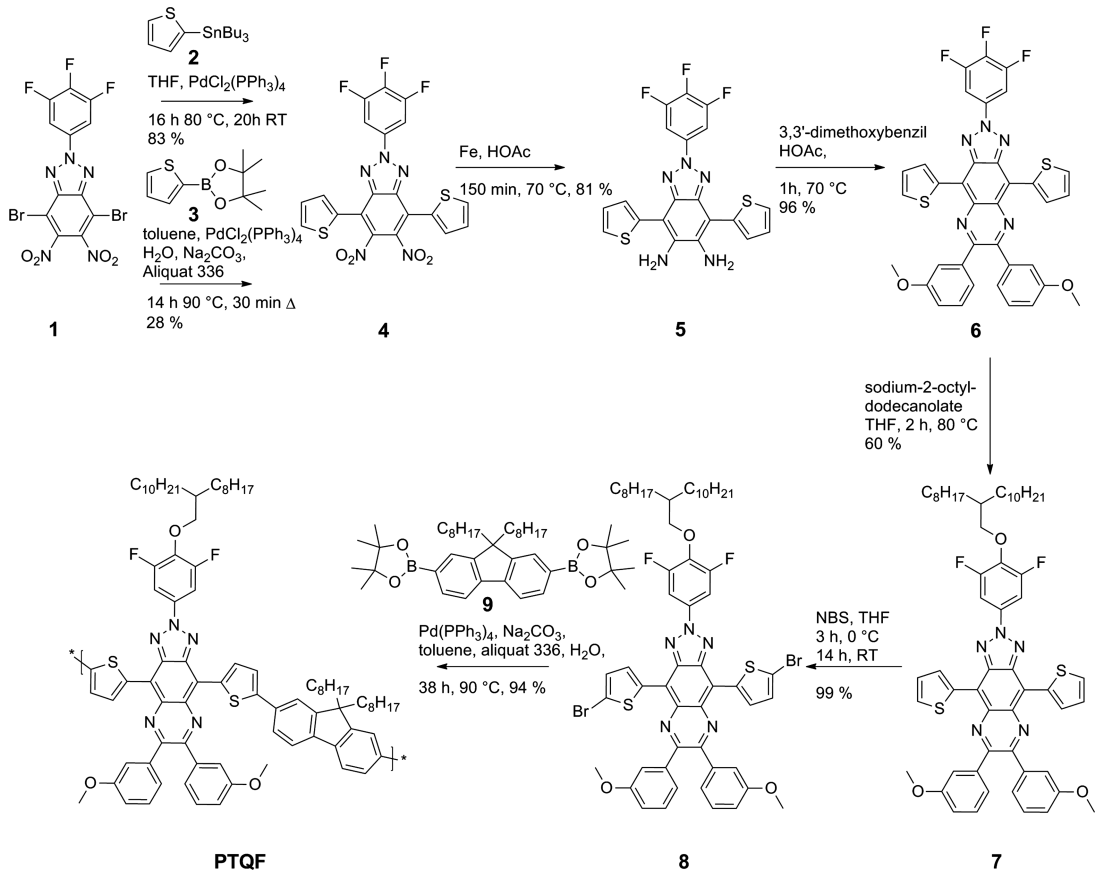

SCHEME 1 Synthetic pathway toward the triazoloquinoxaline-fluorene copolymer PTQF.

it with dioctylfluorene using Suzuki polycondensation method to achieve low band-gap donor material (PTQF) for organic photovoltaics. Here, we report for the first time the use of triazoloquinoxaline as a building block for constructing alternative donor–acceptor low band-gap-conjugated polymers for PSCs.

EXPERIMENTAL

Device Characterization

Bulk heterojunction devices were fabricated using polymers as electron donors and $PC_{61}BM$ (Solenne) as electron acceptor. The standard device structure was as follows: ITO/PEDOT:PSS (AL4083)/polymer:$PC_{61}BM$/Ca/Ag. ITO coated glass with a surface resistance lower than 20 Ω/sq (Osram) was used as transparent electrode. ITO was cleaned by ultrasonic treatment with acetone and isopropyl alcohol and dried under a flow of dry nitrogen. A PEDOT:PSS (AL4083, H.C. Stark) solution diluted in isopropanol was doctor-bladed onto clean substrates, resulting in a thickness of approximately 40 nm as determined with Dektak profilometer. PEDOT:PSS layer was annealed for 15 min at 140 °C in a nitrogen filled glovebox. The active layer consisting of polymers (7 mg/ml) and $PC_{61}BM$ was stirred at 100 °C for 12 h before use and filtered with 0.45-μm PTFE filters. The active layers were doctor-bladed from chlorobenzene solution with 1:2 weight ratio onto PEDOT:PSS layer. A Ca/Ag (20/80 nm) top electrode was evaporated via a mask in vacuum onto the active layers with an electrode area of 0.1 cm^2. PCE was calculated from *J–V* characteristics recorded with Botest source measure unit by an Oriel Sol1A 94061 solar simulator with an intensity of 100 mW/cm^2, where the light intensity was calibrated with a standard silicon photodiode. The external quantum efficiency (EQE) spectra were recorded with a Varian Cary 500 Scan spectrometer with tungsten light source. The hole-only devices with the same active layer thickness as actual devices were fabricated with ITO/PEDOT:PSS bottom contact and PEDOT:PSS/Ag top contact for space charge limited current (SCLC) measurements. A R_s of 4 Ω is considered for the voltage correction; $V = V_{appl} - V_{bi} - V_{rs}$, where V is the effective voltage, V_{appl} is the applied voltage, V_{rs} is the voltage drop, and V_{bi} is the built-in voltage. The hole mobility was calculated by fitting dark $J-V$ curves to SCLC model in which the current density is given by $J = 9\varepsilon_0\varepsilon_r\mu V^2/8L^3$, where ε_0 and ε_r represents the permittivity of the material, μ is the mobility, and L is the thickness of the active layer.

Synthesis and Characterization

The synthesis of the monomers and polymers is shown in Scheme 1. It is based on our earlier triazoloquinoxaline synthesis;[22] however, a change in the order of the different reactions leads to much higher yields. **1** can be coupled with the metallated thiophenes **2** or **3** under Pd-catalysis to give **4**. In this case, the Suzuki coupling gives considerable lower yields than the Stille coupling, which allowed to obtain **4** in 83%

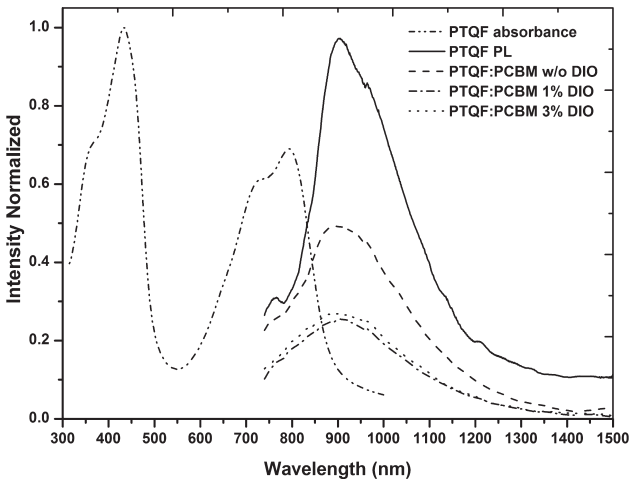

FIGURE 1 UV/vis absorption spectra of PTQF in thin film (..-), PL of pristine PTQF (-), and the PL quenching of PTQF upon addition of $PC_{61}BM$ (—), 1% DIO (-.-), and 3% DIO (...).

yield. Reduction of **4** with iron in acetic acid and subsequent condensation with dimethoxybenzil proceeded in yields of 80 and 96%, deep blue and highly crystalline triazoloquinoxaline **6**. The crystal structure of **6** is presented and discussed in the Supporting Information (Figs. S2 and S3). Treating **6** in THF with a sodium alkoxide leads to nucleophilic substitution of one of the three fluorides and **7** could be obtained in 60% yield. Bromination gave the dibromocompound **8** almost quantitatively. Suzuki polycondensation of **8** to the bispinacol ester of dioctylfluorene bisboronic acid (**9**) and end capping with *p*-tolyl groups gives the corresponding deep green donor–acceptor copolymer PTQF in 94% yield after purification by Soxhlet extraction.

The GPC analysis (vs. PS) shows a M_n of 28 kDa and a polydispersity of 1.6. The DSC (Supporting Information Fig. S4) shows a glass transition at 240 °C, and the polymer shows thermal decomposition with onset temperatures at 360 °C as determined by TGA (Supporting Information Fig. S5).

RESULTS AND DISCUSSIONS

Optical and Electrochemical Properties

Optical and electrochemical properties of a conjugated polymer such as low band gap and high absorption coefficient are crucial to be used in photovoltaics as donor materials. Determination of the absorption and emission peaks and energy levels is one of the key parameters for donor materials to harvest more light and allow energy transfer between donor and acceptor materials. PTQF shows green color in its neutral state.[23] The absorption spectrum of PTQF (Fig. 1) shows two broad absorption peaks at around 400 and 700 nm in thin film that exhibit vibronic progression. The optical band gap of PTQF is calculated as 1.40 eV from the lowest π–π^* transition in the visible region. Compared to its analog P4 (Fig. 2),[24] the optical band gap of PTQF is reduced by 0.68 eV due to the incorporation of the pyrazine moiety to the polymer backbone (Table 1).

PL quenching provides direct evidence for exciton dissociation, which influences the J_{sc} and is used as a measure of donor–acceptor photo-induced charge transfer between the PTQF and $PC_{61}BM$. To understand the degree of quenching, the PL was measured for pristine PTQF and the PTQF:PCBM (1:2) blends with or without DIO. The absorption curves of corresponding films were used to normalize the PL intensity. In Figure 1, the pristine PTQF film shows a strong emission at around 900 nm. The PL spectra of PTQF show only partial quenching upon addition of $PC_{61}BM$ and 1% DIO, which can be a hint of insufficient charge transfer in the blend.

Cyclic voltammetry (CV) of PTQF as thin-film drop cast on a platinum disc electrode shows two major reversible oxidation processes at about 0.6 and 0.8 V versus Fc/Fc^+, thus indicating fast and effective p-doping and de-doping (Supporting Information Fig. S6). Moreover, two reversible reductions occur at about −1.3 and −1.65 V (peak center). The onset potentials for the oxidation and reduction are −1.18 and 0.33 V indicating an electrochemical band gap of 1.51 eV and absolute HOMO and LUMO energies of −5.13 and −3.62 eV, respectively ($E_{1/2}$ (Fc/Fc^+) = −4.8 eV vs. vacuum).

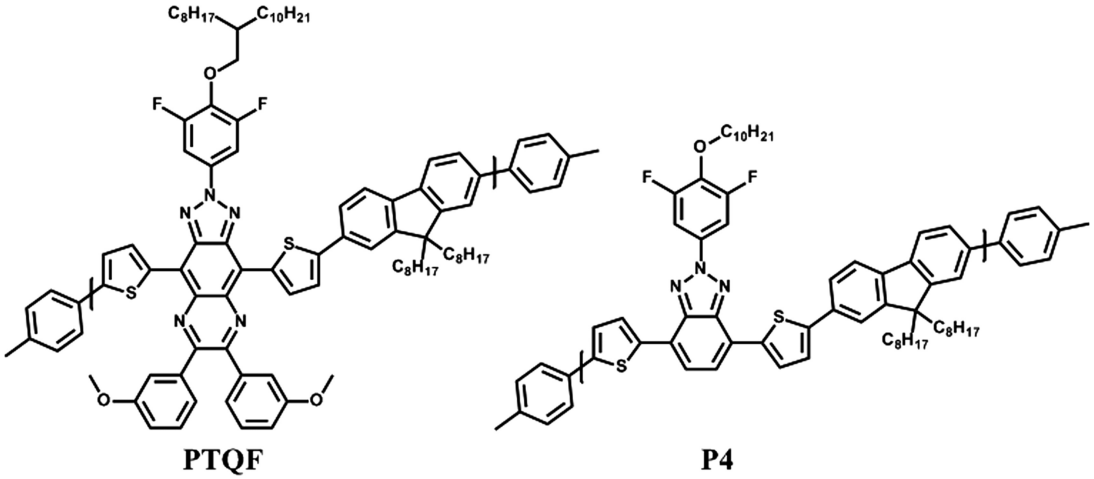

FIGURE 2 Chemical structures of PTQF and P4.

TABLE 1 Optical and Electrochemical Results of P4[24] and PTQF

Polymer	Abs λ_{max} (nm)	Emission λ_{max} (nm)	E_g^{op} (eV)[a]	E_{ox}^{on} (V)[b]	E_{red}^{on} (V)[b]	HOMO (eV)	LUMO (eV)	E_g^{ec} (eV)
P4[24]	547	590	2.08	0.59	−1.44	−5.39	−3.36	2.03
PTQF	790	930	1.40	0.33	−1.18	−5.13	−3.62	1.51

[a] Calculated from the lowest energy in the visible region.

[b] Calculated from CV measurements.

The LUMO–LUMO difference between the polymer and $PC_{61}BM$ is very similar to the exciton binding energy and gives, in combination with the small band gap, a material with an ideal orbital alignment.[25] Table 1 summarizes the electrochemical and optical results for PTQF and its counterpart P4.[24] PTQF revealed much lower oxidation and reduction onsets compared to P4 due to the electron rich pyrazine moiety addition to the backbone. The HOMO energy is increased and LUMO is decreased which results in a lower electrochemical band gap than P4.

Computational Study

To elucidate important structure–properties relations of PTQF, DFT calculations were performed on Model-PTQF that represents a cutout of the respective polymer chain (Supporting Information Fig. S7), where the TQ monomer is flanked on both sides by thiophene as a spacer and a fluorene unit. The HOMO is delocalized all over the thiophene, the fluorene, and the benzo-unit of the triazoloquinoxaline while there is only limited contribution on the triazole and the pyrazine subunit. Contrary, the LUMO is localized mainly on the central part of this polymer excerpt, that is, the thiophenes and mostly the whole triazoloquinoxaline building block, while there is only little contribution on the fluorene parts. These calculations confirm the assumption of a strong CT-character of the HOMO–LUMO transition.

These calculations also give reasonable orbital energies. The HOMO value (−4.37 eV) is about 0.7 eV higher than the experimental value while the LUMO energy (−3.53 eV) fits almost perfectly to the experiment. Therefore, the calculated band gap (0.84 eV) is much smaller than the experimental value. This and the good match for the monomeric precursor **6** (see Supporting Information) could indicate that either the polymer structure is less planar than the calculated one or, more likely, that the cutout of the polymer chain is not appropriate. However, larger cutouts of the polymer chain could not be accurately calculated within a reasonable time span.

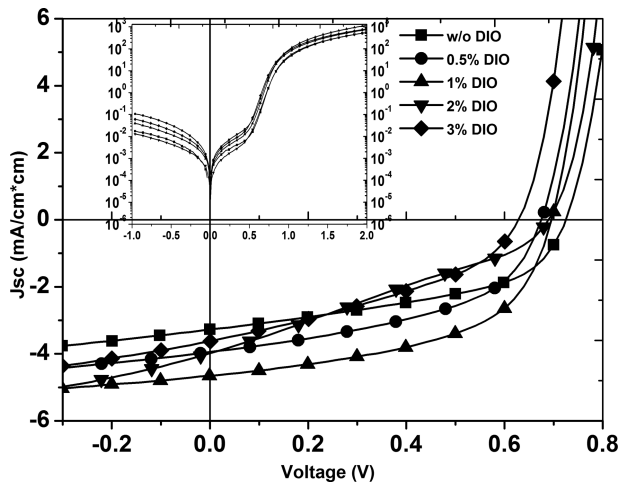

FIGURE 3 Current density–voltage characteristics of PTQF:$PC_{61}BM$ 1:2 devices upon addition of different ratios of 1,8-diiodooctane under dark (inset) and illumination at 100 mW/cm^2.

Photovoltaic Properties

Photovoltaic properties of PTQF were probed on a typical BHJ solar cell architecture with a configuration of ITO/PEDOT:PSS (4083)/polymer:$PC_{61}BM$/Ca (20 nm)/Ag (100 nm). Representative *J–V* curves are shown in Figure 3, and corresponding photovoltaic performances are summarized in Table 2. The cells were optimized with $PC_{61}BM$ using 1:2 (w:w) blend ratio. The solar cells exhibit a V_{oc} of 0.72 V and a power conversion efficiency of 1.13% was achieved with a J_{sc} (3.27 mA/cm^2) without using any additive.

It is known in literature that processing additives such as di(X)octanes[26] as cosolvents (where X can be Br or Cl) are beneficial in creating a morphology of the active layer to achieve high performances. 1,8-diiodooctane (DIO) is used for PTQF:$PC_{61}BM$ 1:2 blend to achieve the desired morphology and domain size to yield higher efficiencies. From Table 2, it becomes obvious that the addition of up to 1% DIO increased the J_{sc} and the overall performance up to 4.65 mA/cm^2 and 1.71%, respectively. However, excess addition of additive strongly affected the V_{oc} and the FF and thus led to inferior PCEs and to a reduced V_{oc} and FF.

Figure 4 displays the EQE for the best device using PTQF:$PC_{61}BM$ 1:2 (w:w) blend upon addition of 1% DIO as photoactive layer. The device exhibits maximum PV response peaks at around 400 and 700 nm, which coincides largely with the absorption spectra of the individual components. The calculated J_{sc} by integrating the spectral response of the

TABLE 2 *J–V* Characteristics of PTQF:$PC_{61}BM$ Device and Effect of the Additive on Device Characteristics

Active Layer	DIO Ratio (%)	V_{oc} (V)	J_{sc} (mA/cm^2)	FF (%)	PCE (%)
PTQF:$PC_{61}BM$	0	0.72	3.27	48.15	1.13
	0.5	0.68	3.94	47.81	1.28
	1	0.70	4.65	52.45	1.71
	2	0.67	3.98	29.02	0.78
	3	0.62	3.62	38.14	0.85

cells agrees well with photocurrent obtained from $J-V$ measurements.

Charge carrier mobility in the blend was measured by the SCLC method. Figure 5 represents the SCLC curves for PTQF:PC_{61}BM blends with and without DIO. Hole mobilities of the PTQF:PC_{61}BM blends without DIO and with 1% DIO are calculated as 4.6×10^{-7} and 1.4×10^{-4} cm^2/V s, respectively, from SCLC measurements. Higher mobility value of PTQF:PC_{61}BM device using 1% DIO also confirms the better performance of the corresponding device.

The impact on the surface morphology by addition of DIO was studied using atomic force microscopy (AFM) (Supporting Information Fig. S8). Tapping mode AFM showed large-scale phase separated domains for the film prepared from PTQF:PC_{61}BM solution without DIO. Nevertheless, with the addition of 1% DIO to the polymer mixture, large clusters disappeared and the length scale of phase separation decreased significantly. Simultaneously, the performance of the solar cell increased. As a consequence of the favored morphology, an increase in J_{sc} and FF was observed for 1% DIO added PTQF:PC_{61}BM films. Addition of excess DIO lead to a microstructure with only limited polymer and fullerene contact area and thus avoid the charge separation within the blend, which resulted in lower V_{oc}, J_{sc}, and FF.

CONCLUSIONS

In conclusion, we report the synthesis, characterization, and implementation of a new triazoloquinoxaline-based fluorene copolymer with low band-gap energy and high V_{oc}. The resulting copolymer was characterized by thermal and spectroscopic methods. A moderate power conversion efficiency of 1.7% was achieved with PTQF:PC_{61}BM devices using 1% DIO. SCLC and AFM measurements confirm that addition of 1% DIO resulted in a more intermixed microstructure of the active layer leading to higher PCEs. The rational design of donor–acceptor copolymers with PTQF using comonomers such as dithienosilole, benzodithiophene, or carbazole may provide organic materials with improved transport and transfer properties yielding OPVs with high efficiencies.

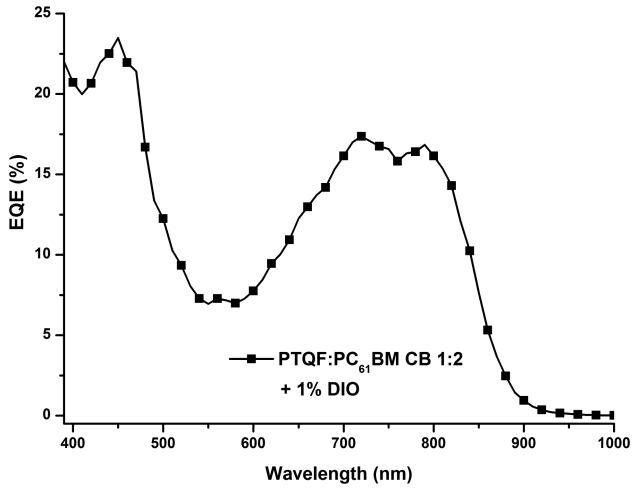

FIGURE 4 EQE curve of the photovoltaic cell with 1:2 PTQF:PC_{61}BM ratio and 1% DIO (v:v).

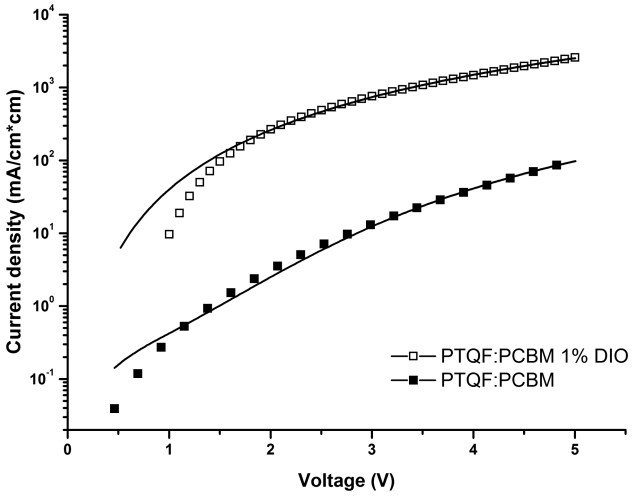

FIGURE 5 Space charge limited currents for ITO/PEDOT:PSS/PTQF:PC_{61}BM/PEDOT:PSS/Ag devices. The lines are the fits for SCLC behavior.

REFERENCES AND NOTES

1 S. C. Price, A. C. Stuart, L. Yang, H. Zhou, W. You, *J. Am. Chem. Soc.* **2011,** *133*, 4625–4631.

2 Y. Liang, Z. Xu, J. Xia, S. T. Tsai, Y. Wu, G. Li, C. Ray, L. Yu, *Adv. Mater.* **2010,** *22*, E135–E138.

3 T. Y. Chu, J. Lu, S. Beaupré, Y. Zhang, J. R. Pouliot, S. Wakim, J. Zhou, M. Leclerc, Z. Li, J. Ding, Y. Tao, *J. Am. Chem. Soc.* **2011,** *133*, 4250–4253.

4 H.-Y. Chen, J. Hou, S. Zhang, Y. Liang, G. Yang, Y. Yang, L. Yu, Y. Wu, G. Li, *Nat. Photon.* **2009,** *3*, 649–653.

5 J. Hou, H.-Y. Chen, S. Zhang, R. I. Chen, Y. Yang, Y. Wu, G. Li, *J. Am. Chem. Soc.* **2009,** *131*, 15586–15587.

6 C. Du, C. Li, W. Li, X. Chen, Z. Bo, C. Veit, Z. Ma, U. Wuerfel, H. Zhu, W. Hu, F. Zhang, *Macromolecules* **2011,** *44*, 7617–7624.

7 M. Zhang, Y. Sun, X. Guo, C. Cui, Y. He, Y. Li, *Macromolecules* **2011,** *44*, 7625–7631.

8 Y. Zhang, J. Zou, H.-L. Yip, K.-S. Chen, D. F. Zeigler, Y. Sun, A. K. Y. Jen, *Chem. Mater.* **2011,** *23*, 2289–2291.

9 S. K. Lee, W.-H. Lee, J. M. Cho, S. J. Park, J.-U. Park, W. S. Shin, J.-C. Lee, I.-N. Kang, S.-J. Moon, *Macromolecules* **2011,** *44*, 5994–6001.

10 O. Inganäs, F. L. Zhang, M. R. Andersson, *Acc. Chem. Res.* **2009,** *42*, 1731–1739.

11 D. Gedefaw, Y. Zhou, S. Hellström, L. Lindgren, L. M. Andersson, F. Zhang, W. Mammo, O. Inganäs, M. R. Andersson, *J. Mater. Chem.* **2009,** *19*, 5359–5363.

12 E. Wang, L. Hou, Z. Wang, S. Hellstrom, F. Zhang, O. Inganäs, M. R. Andersson, *Adv. Mater.,* **2010,** *22*, 5240–5244.

13 E. Wang, L. Hou, Z. Wang, Z. Ma, S. Hellström, W. Zhuang, F. Zhang, O. Inganäs, M. R. Andersson, *Macromolecules* **2011,** *44*, 2067–2073.

14 D. Baran, A. Balan, S. Celebi, B. M. Esteban, H. Neugebauer, N. S. Sariciftci, L. Toppare, *Chem. Mater.* **2010,** *22*, 2978–2987.

15 Y. Dong, W. Cai, X. Hu, C. Zhong, F. Huang, Y. Cao, *Polymer* **2012,** *53*, 1465–1472.

16 Y. Cui, Y. Z. Wu, X. F. Lu, X. Zhang, G. Zhou, F. B. Miapeh, W. H. Zhu, Z. S. Wang, *Chem. Mater.* **2011,** *23*, 4394–4401.

17 A. Balan, D. Baran, G. Gunbas, A. Durmus, F. Ozyurt, L. Toppare, *Chem. Commun.* **2009,** 6768–6770.

18 L. Zhang, C. He, J. Chen, P. Yuan, L. Huang, C. Zhang, W. Cai, Z. Liu, Y. Cao, *Macromolecules* **2010,** *43*, 9771–9778.

19 A. Balan, D. Baran, L. Toppare, *Polym. Chem.* **2011,** *2*, 1029–1043.

20 H. Wettach, F. Pasker, S. Höger, *Macromolecules* **2008,** *41*, 9513–9515.

21 M. F. G. Klein, F. Pasker, H. Wettach, I. Gadaczek, T. Bredow, P. Zilkens, P. Vöhringer, U. Lemmer, S. Höger, A. Closmann, *J. Phys. Chem. C,* **2012,** *116*, 16358–16364.

22 F. M. Pasker, S. M. Le Blanc, G. Schnakenburg, S. Höger, *Org. Lett.* **2011,** *13*, 2338–2341.

23 S. Ozdemir, M. Sendur, G. Oktem, Ö. Doğan, L. Toppare, *J. Mater. Chem.* **2012,** *22*, 4687–4694.

24 F. M. Pasker, M. F. G. Klein, M. Sanyal, E. Barrena, U. Lemmer, A. Colsmann, S. Höger, *J. Polym. Sci. Part A: Polym. Chem.* **2011,** *49*, 5001–5011.

25 M. C. Scharber, D. Mühlbacher, M. Koppe, P. Denk, C. Waldauf, A. J. Heeger, C. L. Brabec, *Adv. Mater.* **2006,** *18*, 789–794.

26 S. J. Lou, J. M. Szarko, T. Xu, L. P. Yu, T. J. Marks, L. X. Chen, *J. Am. Chem. Soc.* **2011,** *133*, 20661–20663.